Power Modeling and Exploration of Dynamic and Partially Reconfigurable Systems

Robin Bonamy, Sébastien Bilavarn, Daniel Chillet, Olivier Sentieys

Power Modeling and Exploration of Dynamic and Partially Reconfigurable Systems

ROBIN BONAMY[1], SÉBASTIEN BILAVARN[2], DANIEL CHILLET[1], AND OLIVIER SENTIEYS[1]

[1]CAIRN, University of Rennes 1, CNRS, IRISA
[2]LEAT, University of Nice Sophia Antipolis, CNRS

Although fairly known for a long time, the vast potential of Dynamic and Partial Reconfiguration (DPR) for high energy efficiency is still difficult to exploit, for reasons that are more methodological than purely technical. This work addresses this problem and provides a contribution by seeking to improve energy efficient deployment and analysis for embedded heterogeneous multiprocessor platforms representative of current and upcoming systems. This paper explores the potential energy efficiency improvements of DPR on the concrete implementation of a H.264/AVC video decoder. The methodology used to explore the different implementations is presented and formalized. This formalization is based on pragmatic power consumption models of all the tasks of the application that are derived from real measurements.

Results allow to identify low energy / high performance mappings, and by extension, conditions at which partial reconfiguration can achieve energy efficient application processing. The improvements are expected to be of 57% in energy and 37% in performance over pure software execution, corresponding also to 16% energy savings over static implementation of the same accelerators for 10% less performance.

1. INTRODUCTION

Minimizing power consumption and extending battery life are major concerns in popular consumer electronics like mobile handsets and wireless handheld devices. Silicon chips embedded in these products face challenging perspectives with the rise of processing heterogeneity introduced to address heat and power density problems. Efficient methodologies and tools are thus necessary to help the mapping and execution of applications on such complex platforms considering high demands for performance at less energy costs.

In parallel, in the context of mobile devices, video decoding is known as part of intense computation, which leads to an important impact on energy consumption. Considering this context and the need of methodologies to help the designers of such systems, it is essential that a subset of relevant solutions can be quickly identified and evaluated from early steps of development. This process usually relies on high level modeling and estimations to help analyzing many complex interactions between a variety of implementation choices. To address this topic, performance models of FPGAs have been widely defined and proposed but power consumption has been less investigated in comparison, especially regarding Dynamic and Partial Reconfiguration (DPR).

DPR is a feature introduced to further improve the flexibility of reconfigurable based hardware accelerators. It exploits the ability to change the configuration of a portion of a FPGA while other parts are still running. By sharing the same area for the execution of different sequential tasks, DPR allows reducing the size of active programmable logic required for a given application [1][2]. Therefore, improving the area efficiency also results in decreasing static power consumption which is directly linked to the number of transistors in the chip. The counterpart is that an additional part of power is needed to switch from a current configuration to the next one. Thus, this DPR cost needs to be properly assessed and analyzed in order to check if there is an actual power consumption benefit at the complete system level, for a given application. This paper investigates the exploitation of this on a relevant case study addressing the

implementation of a H.264/AVC video decoder in search of the best global energy efficiency at the complete system level. From this concrete example, we define a pragmatic formalization of the problem that can be used to analyze mapping combination of tasks on hardware and software units with DPR, and to provide reliable evaluations of execution time, area, power and energy. In particular, it is shown how the different model parameters are defined, applied and exploited based on a real-life deployment study and from the deriving possible power measurement and breakdown analysis opportunities. The defined power characterization strongly grounded in experimentation therefore is shown to ensure applicability and relevance of the proposed software / DPR hardware energy modeling scheme and to afford the ability to produce pertinent estimation numbers of DPR benefits from large system level exploration based on its use.

The paper firstly presents state of the art techniques in the general field of dynamic reconfiguration in Section 2, with a special emphasis on energy analysis and optimization. Then Section 3 details formal models for application, platform and dynamic reconfiguration underlying the mapping analysis of the H.264/AVC decoder. The automatic analysis of different mappings and scheduling of hardware and software application tasks is described in Section 4. Then, a result analysis of the full video application deployment is presented along with estimation values that are discussed in Section 5. Finally, we conclude the paper and suggest future directions for research.

2. DYNAMIC PARTIAL RECONFIGURATION AND EN-ERGY EFFICIENCY

A. Energy efficient DR systems

Embedded systems have to cope with numerous challenges such as limited power supply, space and heat dissipation. Extensive research efforts are currently carried out to address these problems. For low production volumes, reconfigurable architectures and FPGAs have been attractive in embedded systems due to their flexibility, allowing faster development at lower costs than Application Specific Integrated Circuits (ASICs). However, the energy efficiency and the maximum frequency of reconfigurable hardware are also impaired by their flexible interconnect which does not allow to reach the power and performance levels of custom ASICs [3, 4].

As the focus of this work is on energy aware analysis of dynamic and partially reconfigurable systems, power modeling is central to the problem. One can find a variety of works spanning the general field of Dynamic Reconfiguration, among which a few primarily address power and energy efficiency concerns. Among relevant works, [5] presents an approach that investigated power management for Reconfigurable Video Coding (RVC) involving coarse grained reconfigurable systems. As far as DPR is not concerned, power estimations are based on SoC libraries and power issues reported here are quite specific to the RVC methodology and cannot be directly extended to FPGA and DPR implementations. In [6] an evolvable hardware system is used to optimize the power consumption of a DPR platform at run time. A singularity of this method is that the search space is explored at run time from measured power consumption profiles to adapt the genes of an evolutionary algorithm. However results reported are 5% to 10% battery lifetime benefits and no further energy analysis is provided. The approach in [7] describes an architecture exploration of hardware-based processing units with DPR support integrated in an OpenCL framework. Despite the undeniable interest of addressing an

important weak point of reconfigurable hardware (programming model), support for the OpenCL programming mode in the study overshadow energy analysis and results and do not provide yet relevant DPR power and energy efficiency concerns.

From these relatively few number of works, it can be observed that all fall into delineated perimeter of applications. A large majority focuses on hardware accelerators (leaving aside the questions of software units) and none deal with both FPGA reconfiguration (DPR) and software execution. Many works address relatively simple applications and face the difficult problem of power analysis. Therefore, it can be said that the exploitation of energy efficiency for DPR systems still lacks of a solid grasp of the complex mapping opportunities for representative computing (multiprocessor) platforms, and this is mainly due to a global power modeling problem. As there is up to our knowledge, not much study addressing explicitly the definition of abstract power models, we describe in the following a set of studies that nonetheless provide valuable insights on the exploration of DPR based solutions in terms of energy efficiency.

B. DPR related techniques for energy efficiency

DPR allows a better use of hardware resources by sharing and reusing reconfigurable regions (PRRs) during execution, thus less area and energy consumption are expected. A variety of other techniques can be associated to this inherent DPR capability. For instance, it is possible to clear the configuration data of a PRR (referred to as *blank configuration* in the following) when it is unused which leads to decrease the share of static power associated with PRRs [8]. As an important part of power consumption also comes from clock signals, some techniques investigated the use of dynamic reconfiguration to reduce clock related impacts. A low overhead clock gating implementation based on dynamic reconfiguration has been proposed in [9], achieving 30 % power reductions compared to standard FPGA clock-gating techniques based on LUTs. Another approach has been developed to modify the parameters of clock tree routing at run time reconfiguration to moderate clock propagation in the whole FPGA and decrease dynamic power [10]. Finally, self-reconfiguration also permits online modification of clock frequency with low resource overhead by acting directly on clock management units from the reconfiguration controller [11].

Dynamic and partial reconfiguration faces the difficult problem of task placement, both spatially on reconfigurable regions and temporally in terms of scheduling. Therefore DPR demands specific requirements to support this type of execution. It is generally the responsibility of a task scheduler, like [12], to decide online which resource will support the execution of a task. The question becomes even more critical when addressing context saving issues related to the preemption and relocation of hardware tasks as discussed for example in [13]. In terms of power, scheduling must state when task reconfiguration occurs such as to avoid unnecessary idle consumption prior to execution [14]. It is also responsible for choosing to use *blank* configurations or not while ensuring this decision actually leads to an overall energy gain [15].

Another important element in DPR optimization is related to hardware implementation and parallelism. Parallelism has the potential to drastically decrease the execution time of a hardware implementation. A technique to exploit this potential is to apply code transformations such as those available in High Level Synthesis (HLS) tools. Previous works reported two times energy reductions between sequential and unrolled loops of a hardware matrix multiplication implementation [16]. This par-

allelism exploitation is especially relevant for DPR since it can help the adaptation of a better area power performance tradeoff at run time.

However, all these opportunities add many dimensions to the DPR implementation problem for which there are currently few design analysis support, especially concerning energy and power consumption. It is thus extremely difficult to i) identify the most influential parameters in the design and ii) understand the impact of their variations in search of energy efficiency. In the following, we detail the deployment analysis of a H.264/AVC decoder on a representative performance execution platform (multicore with DPR), and in the most energy efficient way. To support this, we present first a formal model of application, platform and mapping to allow a more systematic exploration and evaluation of their associated impacts. Relevant power and energy models of DPR represent another essential condition to provide early reliable evaluations. The power and energy models that are used in the proposed exploration are based on actual measurements of the DPR process which are further described in [17]. Finally, a greedy exploration heuristic is made out of this base and described in details. It is shown in the result analysis how a set of relevant energy and performance tradeoffs can be identified and compared against characteristic solutions (best performance, static hardware, full software execution, etc.).

3. PROBLEM MODELING

Previous work addressed a detailed study of DPR energy modeling which led to identify significant parameters of dynamic reconfiguration (FPGA and PRRs idle power, DPR control) [17]. This section fully extends the model to support a full and realistic platform (hardware, software execution units), application (hardware, software tasks) and mapping characterization which is defined from a set of actual power values measured on real platforms reported in section B and C. Therefore the assessment (i.e. practical applicability) of the proposed global modeling scheme is shown on a H.264 video decoder for an assumed dual core reconfigurable platform (CortexA8/Virtex-6 LX240T).

A. Target platform model

As previously stated, the target platform is a heterogeneous architecture that can be composed of processors and dynamically reconfigurable accelerators. Each type of execution unit is formalized by a set of specific parameters that captures all the information needed for deployment exploration. These parameters can be broadly classified in three categories that are listed in Table 1: platform topology, execution units and dynamic and partial reconfiguration characterization.

A.1. Platform topology

Execution Units (EU) are divided in two categories: software and hardware execution units. The system is supposed to be made of a number N^{core} of software execution units (processor cores) and N^{PRR} hardware execution units. The hardware execution units are defined as the partially reconfigurable regions of the FPGA. Therefore, the total number of hardware and software execution units N^{EU} in the architecture is $N^{core} + N^{PRR}$, and the jth execution unit of the architecture is tagged by EU_j with $j \in [1, N^{EU}]$. In this abstract representation, a heterogeneous SoC platform is represented by the set of all its execution units $\{EU_j\}$ and this composition is considered fixed at run-time.

Table 1. Parameters used for heterogeneous architecture formalization

Variable	Range	Definition
N^{core}	$\in \mathbb{N}^*$	Number of software execution units
N^{PRR}	$\in \mathbb{N}^*$	Number of hardware execution units
N^{EU}	$= N^{PRR} + N^{core}$	Total number of execution units
EU_j	$\forall j = 1, ..., N^{EU}$	The jth execution unit
SoC	$= \{EU_j\}$	A platform is a set of execution units
N_j^{freq}	$\in \mathbb{N}^*$	Number of frequencies for software EU_j
$F_{j,k}$	$\forall k = 1, ..., N_j^{freq}$	The kth frequency of software EU_j
$P_{j,k}^{empty}$	$\in \mathbb{R}^+$	Empty power consumption for software EU_j at $F_{j,k}$
$P_{j,k}^{run}$	$\in \mathbb{R}^+$	Running power consumption for software EU_j at $F_{j,k}$
N_j^{cell}	$\in \mathbb{N}^*$	Number of logic cells for hardware EU_j
N_j^{bram}	$\in \mathbb{N}^*$	Number of RAM blocks for hardware EU_j
N_j^{dsp}	$\in \mathbb{N}^*$	Number of DSP blocks for hardware EU_j
P_j^{empty}	$\in \mathbb{R}^+$	Empty power consumption for hardware EU_j
T^{1cell}	$\in \mathbb{R}^+$	Time required to reconfigure one logic cell
E^{1cell}	$\in \mathbb{R}^+$	Energy required to reconfigure one logic cell

A.2. Execution units

The size of a hardware unit EU_j is characterized in terms of logic resources with parameters N_j^{cell}, N_j^{bram} and N_j^{dsp} to ensure realistic resource representation. The *cell* terminology refers to the main configurable resource of the programmable logic (e.g. Xilinx Slices, Altera Logic Elements).

Concerning the power model, a distinction is made between different components of each EU_j. The empty power consumption, P_j^{empty} or $P_{j,k}^{empty}$, reflects the power consumed when no application task is loaded, respectively for PRRs and cores (at frequency $F_{j,k}$). It is worth noting concerning PRRs that a task configured on it accumulates two contributions: $P_{i,k}^{idle}$ when the task is idle, and $P_{i,k}^{run}$ when it is running, which are both implementation dependent and therefore described in the Section B.3. The characterization of P_j^{empty} is additonally useful to consider PRR blanking opportunities in the analysis of task deployments. For software units, $P_{j,k}^{run}$ is the power of a core EU_j running at $F_{j,k}$ (full load). The energy of a software task can then be computed from $P_{j,k}^{run}$ and the corresponding execution time.

A.3. Dynamic and partial reconfiguration

Taking into account the cost of dynamic and partial reconfiguration involves two types of overhead: delay and energy. As the reconfiguration delay is mainly dependent on the speed of the reconfiguration controller and size of the configuration bitstream, it can be efficiently described by parameter T^{1cell} representing the time needed to configure one logic cell and reflects the performance of the reconfiguration controller. Power is addressed in a similar way by parameter E^{1cell} reflecting the energy needed to configure one logic cell. As configuration depends mostly on the number of logic cells composing a PRR in practice, delay and energy overheads are fairly easy to compute.

B. Application power and mapping model

Different features of the application tasks need to be known for exploration and estimation. These characteristics are formalized by a set of parameters that are exposed in Table 2 and that can be

classified in three categories: task graph, task implementations and task execution characterization.

Table 2. Parameters used for application formalization

Variable	Range	Definition
N^T	$\in \mathbb{N}^*$	Number of tasks of the application
T_i	$\forall i = 1, ..., N^T$	The ith task of the application
$\mathcal{G}$	$= \{T_i\}$	Task-dependency graph
$T^{eq}_{i1,i2}$	$\in \{0,1\} \; \forall i1, i2 = 1, ..., N^T$	Tasks equivalence matrix
N^{imp}_i	$\in \mathbb{N}^*$	Number of implementations of T_i
$T_{i,k}$	$\forall k = 1, ..., N^{imp}_i$	The kth implementation of T_i
$I_{i,j,k}$	$\in \{0,1\}$	Defines if $T_{i,k}$ is instantiable on EU_j
$C_{i,j,k}$	$\in \mathbb{R}^+$	Execution time of $T_{i,k}$
$E_{i,j,k}$	$\in \mathbb{R}^+$	Energy consumption of $T_{i,k}$ on EU_j
$P^{idle}_{i,k}$	$\in \mathbb{R}^+$	Idle power consumption of $T_{i,k}$
$P^{run}_{i,k}$	$\in \mathbb{R}^+$	Running power consumption of $T_{i,k}$

B.1. Task graph

A task-dependency graph $\mathcal{G}$ is used to reflect execution concurrency in the mapping problem. The dependencies between tasks are enumerated by an adjacency matrix representation which is convenient to process by an analysis algorithm. The adjacency matrix is a $N^T \times N^T$ matrix used to represent dependencies between tasks. Considering a row i, the value in each column is 1 if T_i is dependent on the task represented by the column index, otherwise this value is 0. This adjacency matrix is asymmetric and -1 values are used to represent an inverted edge direction of the graph (Figure 1). In addition, the adjacency matrix is completed with another information called the task equivalence matrix $T^{eq}_{i1,i2}$, which is used to indicate the identicalness of two or more tasks, meaning that they have the same execution code or bitstream. This is useful to minimize execution units and improve their utilization rate, which is an important condition for DPR efficiency as it will be pointed out in the results.
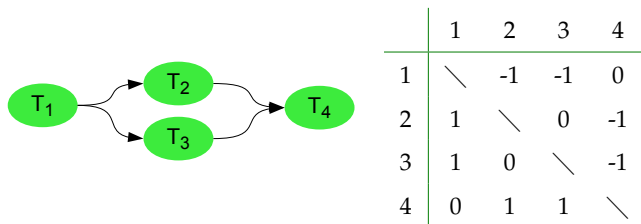

Fig. 1. Simple graph task example and it's associated adjacency matrix.

B.2. Task implementations

From previous representation, it is also required to describe the possible implementations for each task. As we aim to explore combinations of mappings to the execution units, various implementations of the same task can be described. Different software (CPU core, frequency) and hardware (PRR) implementations can be specified to reflect several power performance tradeoffs in the exploration. The total number of possible hardware and software implementations for task T_i is N^{imp}_i, and $T_{i,k}$ is used to represent the kth implementation of task T_i with $k \in [1, N^{imp}_i]$.

B.3. Task execution

First, a variable $I_{i,j,k}$ is used to express if $T_{i,k}$ can be executed using EU_j (0 false, 1 true). When task T_i is running on a software execution unit (EU_j at frequency $F_{j,k}$), the corresponding execution time and energy consumption are defined by $C_{i,j,k}$ and $E_{i,j,k}$. Energy can be derived from the power characterization of a CPU core: $E_{i,j,k} = P^{run}_{j,k} * C_{i,j,k}$.
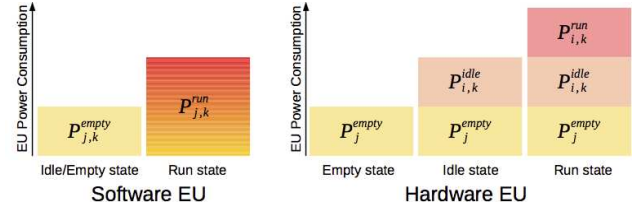

Fig. 2. Power contributions of an execution unit.

A slightly different model applies for hardware tasks (Figure 2). When the kth implementation of a hardware task is mapped to a PRR, it comes with a part of idle power. This contribution is referenced by $P^{idle}_{i,k}$ for the kth implementation of task T_i. The remaining power contribution $P^{run}_{i,k}$ is added when the task is running. Therefore, the total power of PRR EU_j when $T_{i,k}$ is configured and running is $P^{idle}_{i,k} + P^{empty}_j + P^{run}_{i,k}$.

C. Model assessment

We apply previous modeling on the H.264 decoder in a way to evaluate the extent of the formalization defined and show the actual setting of model parameters from a clear measurement process. In the absence of an available platform supporting all features necessary for these investigations (multiprocessor, power measurement, DPR, Linux, DVFS, etc.) at the beginning of this work, this characterization example is based on a dual CortexA8/Virtex-6 LX240T assumed platform. Power model parameters were set upon physical measurements on a Mistral Texas Instruments TI OMAP 3530 EVM (65nm) board for software cores and a Xilinx EK-V6-ML605-G (40nm) board for DPR acceleration. Further details of the specification graph and functions of the video decoder are given in Section 5.

C.1. Power measurement procedure

The FPGA device which is addressed in the following of this study is a Xilinx Virtex-6 LX240T. All measurements to set up the different parameters of the models are thus made on a Xilinx ML605 platform, including a built-in shunt resistor that can let us monitor the current through the FPGA core.
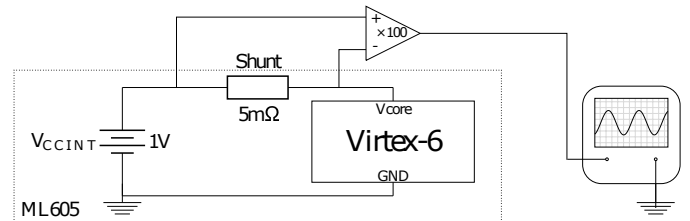

Fig. 3. Current measurement schematics on ML605 Board using a high-precision amplifier.

Figure 3 shows the experimental setup for power measurements. We use the Virtex core shunt with a high-precision amplifier to handle current and power measurements that are logged

with a digital oscilloscope. This setup allows to measure dynamic variations of current and power consumptions as low as milliamps and milliwatts during the execution of the device.

C.2. Platform

A first issue is to determine a set of relevant PRRs in terms of number (N^{PRR}) and size (N_j^{cell}, N_j^{bram}, N_j^{dsp}). We do not handle this partitioning in our approach and rely on the methodology of [18] which defines a systematic approach to achieve this. Then, the empty power of PRRs (P_j^{empty}) can be derived from the empty power per logic cell, which is the power that can be measured when the full FPGA is powered but does not contain any configuration (at voltage and internal temperature constant), averaged by the number of cells. For instance, the Virtex-6 device used has a measured empty power of $1.57W$ (at $1V$, $35°C$) for a capability of 37680 slices, which leads to a parameter of $41.7 \ \mu W/slice$. It is then easy to derive the empty power of a PRR from its size. The configuration of a task on a PRR also adds contributions that are implementation dependent ($P_{j,k}^{idle}$, $P_{i,k}^{run}$), the determination of these parameters is thus described in the following section.

Empty and running power of CPU cores come from similar measurements. It is worth noting here that the model let the specification of different types of cores and frequencies ($F_{j,k}$). A software implementation can be associated to a core frequency k in this case. $P_{j,k}^{empty}$ and $P_{j,k}^{run}$ are the consumptions measured respectively when the core is idle (no application task) and running (assuming 100% CPU load). As an illustration, these values are $24mW$ and $445mW$ for an OMAP3530 based platform operating at 600MHz [19].

The power model used for DPR reconfiguration is the *Coarse Grained DPR estimation model* detailed in [17]. In the example of Section B, this model is calibrated for an optimized reconfiguration controller called UPaRC [20] supporting $400 \ MB/s$ at an average power of $150 \ mW$. The minimum reconfiguration region in a Virtex-6 device (one $cell = one \ slice$) is one frame, where one frame is 324 bytes and contains two slices [21]. In these conditions, the corresponding T^{1cell} is $(324B \ / \ 400MB/s) \ / \ 2 = 0.41 \ \mu s$. In addition, the related E^{1cell} is $T^{1cell} \times 150 \ mW = 61.5 \ nJ$. From these values, it is convenient to derive reconfiguration delay and energy for PRRs of different shapes and sizes.

C.3. Application

In the formalism of Table 2, hardware and software task mapping parameters can be settled by defined implementations and measures. Classical profiling can be used to set out software execution time $C_{i,j,k}$ and derive the associated energy cost $E_{i,j,k}$ from the power $P_{j,k}^{run}$ of the executing core at frequency k (e.g. $E_{1,1,1} = 445mW * 5ms = 2.23mJ$ for T_1 on core EU_1 in Table 5).

As for hardware tasks, they are fully generated using an ESL (Electronic System Level) methodology described in [22]. Hardware mapping parameters are derived from measurements made possible by full accelerator implementation. $P_{i,k}^{idle}$ is the consumption measured when $T_{i,k}$ is configured but not running. This power is supposed to be independent from PRRs in our model. $P_{i,k}^{run}$ is the fraction of dynamic power added when $T_{i,k}$ is running (also supposed independent from PRRs), that can be determined in practice by subtracting the consumption of a configuration where $T_{i,k}$ is running from the consumption of a configuration where $T_{i,k}$ is idle. Therefore, the total power of a hardware task T_i is the sum of P_j^{empty} of a PRR and $P_{i,k}^{idle}$ when the task is idle, plus an additional contribution $P_{i,k}^{run}$ when the

task is running. For example, the first hardware implementation $I_{5,4,2}$ of $T_{5,2}$ on EU_4 (PRR2) in Table 5 has a total energy cost $E_{5,4,2}$ computed from P_4^{empty} of PRR2, $P_{5,2}^{idle}/P_{5,2}^{run}$ of $T_{5,2}$, and the corresponding execution time $C_{5,4,2}$:

$$
\begin{aligned}
E_{5,4,2} &= (P_4^{empty} + P_{5,2}^{idle} + P_{5,2}^{run}) * C_{5,4,2} \\
&= (137mW + 34.2mW + 11.47mW) * 2.46ms \\
&= 0.45mJ.
\end{aligned}
$$

This view is actually integrated in a more global framework for power modeling and analysis called Open-PEOPLE [23]. In particular, the open power platform supports remote measurements and therefore let the definition of previous parameters reducing the need for equipment, devices and the usually complex monitoring procedures associated. The following section shows how using previous models developed from a set of acurate and concrete measurements can help defining relevant and reliable deployment exploration analysis.

4. DEPLOYMENT ANALYSIS

Based on previous modeling and formalization, more methodological approaches can be defined to explore the mapping space and provide relevant evaluations. Execution time, area (in terms of programmable logic resources), energy and power profiles can be computed from the full characterization of the system available, including description and power models of execution units, SoC platform, Hw/Sw implementations of tasks, Dynamic Partial Reconfiguration and Partial Reconfigurable Regions. Figure 4 depicts the exploration methodology used for this energy efficiency study, and is further detailed in the following.

A. Exploration inputs

A.1. System description

The estimation flow starts with descriptions of application tasks and execution resources (Figure 4-1-). Tasks dependencies are specified using the aforementioned task-dependency graph ($\mathcal{G}$, N^T, T_i, $T_{i1,i2}^{eq}$), which is further processed using graph traversal techniques. Platform resource information like the size, number of PRRs and CPUs must be considered to determine different possible allocations. We assume here that the definitions of PRRs have been done so far (Section C.2). Hw/Sw implementations of tasks and SoC platform characteristics required to compute power estimations come from specific libraries that are described in the following.

A.2. SoC libraries

Power consumption and execution time of tasks for each possible execution unit are described in *Tasks Implementation libraries* (Figure 4-2-). For hardware tasks, these settings can be estimated by hardware dedicated power estimators, like the Xilinx Power Estimator, and execution time can be derived from timing reports produced by high level synthesis. Energy of software tasks can also be based on measurements or derived from data released by processor manufacturers. However for the sake of precision, power and execution times in the following come from real implementation and measurement for both hardware and software tasks (Section C.3).

Specific power and energy models are used to estimate the overheads resulting from PRR reconfigurations. These models have enough accuracy to estimate the latency, energy, and power profile of a reconfiguration from the characteristics of the reconfiguration controller, PRR and tasks involved [17].
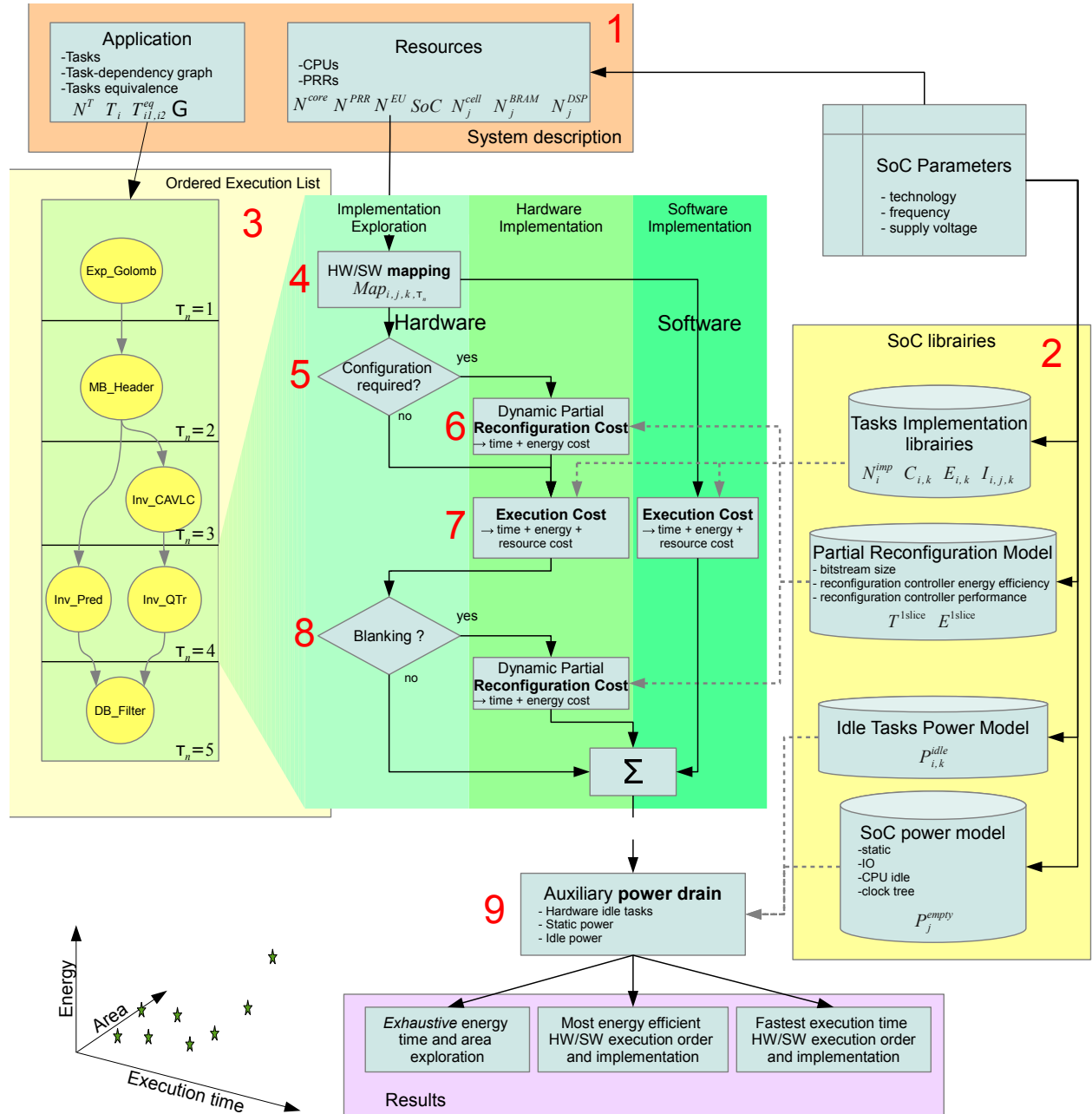
Fig. 4. Global exploration and power / performance estimation flow.

Table 3. OEL parameters used in exploration

Variable	Range	Definition
N^{OEL}	$\in \mathbb{N}^*$	Number of OELs extracted from $\mathcal{G}$
N_n^{TS}	$\forall n = 1, ..., N^{OEL}$	Number of time slots in the nth OEL
τ_n	$= 1, ..., N_n^{TS}$	Current time slot of the nth OEL
$OEL_{\tau_n, i}$	$\in \{0,1\}$	Presence of T_i for τ_n

Another aspect in the estimation model is the power consumed by a hardware task present on a PRR, but not in use (idle power). An idle task power model is used to compute this contribution from sizes of tasks and PRRs. An improvement here is to configure a PRR with an empty task to reduce the associated idle power. This possibility is included in the mapping exploration process (Figure 4-8-).

Finally, device parameters such as the size, process technology and external adjustments like voltage and frequency are also present in *SoC Parameters*. This type of information is not currently used in the computation of estimations. Since previous libraries have been derived from measurements on a specific device (Virtex-6), we kept these characteristics in a way to derive implementations and models for different technologies.

B. Ordered execution lists

Scheduling and allocation must be known in order to compute performance and energy estimations. We use information derived from the task-dependency graph to define a preliminary order for the execution of tasks. This is the role of the Ordered Execution List (OEL), which is a list of tasks similar to the task graph except that it sequentially determines which tasks must be launched for a time slot (τ_n). Each time slot corresponds to the end of a task and the beginning to, at least, one other task. The OEL is a representation of a static task schedule which is useful to derive at low complexity a number of feasible deployments. This ensures keeping enough workstation capacity to process the analysis of extensive task mappings along with fine complete power characterizations.

However, one OEL is not always enough to cover the best scheduling solution, especially if the application supports a lot of parallel tasks. An example is shown in Figure 4-3- where tasks *Inv_Pred* and *Inv_QTr* are executed in the same time slot, whereas *Inv_Pred* could also be run in parallel with *Inv_CAVLC*. In such a case, several OELs can be extracted from $\mathcal{G}$ and explored one by one. The mapping definition process from an OEL depends on the formal parameters of Table 3 and is further described in the next section.

C. Mapping exploration

C.1. Implementation selection

For each task beginning at the current time slot τ_n, an implementation is selected from the list of possibilities (hardware or software) available in the task implementation library (Figure 4-4-). Map_{k,i,j,τ_n} is a variable which represents the implementation choice by its value: 1 at τ_n when $T_{i,k}$ is mapped on EU_j. This variable is also set under the following constraints:

- one task is mapped only once

$$\sum_{j,k,\tau_n} Map_{k,i,j,\tau_n} = 1 \quad \forall i \in 1, ..., N^T \tag{1}$$

- one EU can run only one task at the same time

$$\sum_{i,k} Map_{k,i,j,\tau_n} \leq 1 \tag{2}$$

$$\forall j \in 1, ..., N^{EU}, \forall \tau_n \in 1, ..., N_n^{TS}$$

For a mapping choice expressed by *Map*, estimations of power and execution time are then computed subsequently.

C.2. Partial reconfiguration cost

Reconfiguration is likely to occur when a task is mapped on a hardware execution unit (PRR), except if this task is already configured on this PRR (Figure 4-5-). In the situation where a reconfiguration is needed (Figure 4-6-), time and energy overheads are computed respectively by:

$$T_j^{conf} = T^{1cell} \times N_j^{cell} \tag{3}$$

$$E_j^{conf} = E^{1cell} \times N_j^{cell} \tag{4}$$

It is worth noting here that, although BRAM and DSP blocks are involved in computing the use of FPGA resources (section 3.1.2), they are not considered in the cost of reconfiguration control because it would incur low level layout and device dependent considerations for relatively few accuracy benefit (reconfiguration is a fraction of hardware task execution).

C.3. Task execution cost

Contributions of the actual execution of tasks (hardware and software) are then added to previous cost estimation (Figure 4-7-). The execution time for the current implementation of task T_i is given by $C_{i,j,k}$ while the energy consumption for this implementation is defined by $E_{i,j,k}$.

C.4. Blanking analysis

When a hardware resource is not used for some time, blanking is an opportunity that can also be considered to save power (Figure 4-8-). However this technique comes with an added cost that has to be estimated [15]. This is determined by comparing the energy with and without blanking using the following expressions:

$$E_j^{blanking} = E_j^{conf} + E_j^{empty}$$

$$= E_j^{conf} + P_j^{empty} * (T_j^{idle} - T_j^{conf}) \tag{5}$$

$$E_{i,j,k}^{idle} = P_{i,k}^{idle} * T_j^{idle} \tag{6}$$

where T_j^{idle} is the time during which EU_j is idle, waiting for a new task to begin. If $E_j^{blanking} < E_{i,j,k}^{idle}$ then blanking is an acceptable solution.

D. Auxiliary power drain

Auxiliary power contributions are also considered to fully characterize the energy consumption (Figure 4-9-). These contributions are from the static leakage power and from the idle power of the clock tree, both considered in $P^{SoCidle}$. The portion of power consumed by the execution units even when they are not in use ($P_{j,k}^{empty}$) is also added. We consider that power of a blank PRR is included in P_j^{empty}. However, hardware tasks already configured and idle also lead to power drains that are considered ($P_{i,k}^{idle}$)
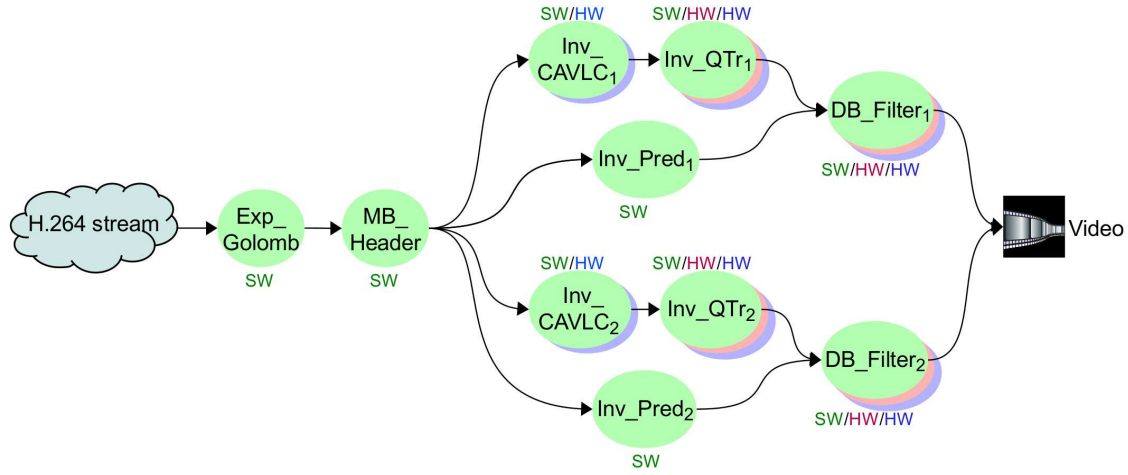
Fig. 5. H.264 decoder task flow graph.

E. Global cost characterization

At the end of an OEL analysis, energy contributions and execution times are added for each global mapping solution. An exhaustive search is currently used to enumerate the possible deployments of tasks on the execution units. This process consists in generating progressively at each time slot different branches for the OEL mapping. The end of a branch corresponds to a global deployment solution with its associated estimation of energy, area (resources) and performance. Notable solutions minimizing energy or performance are highlighted from a scatter plot representation of the results to help comparing the mappings explored (Figure 6). Scheduling and the corresponding power profiles are computed as well to further analyze and implement a particular solution, as illustrated in Figure 8. Next section outlines these results that are derived from the application to a parallelized accelerated H.264/AVC decoder.

5. APPLICATION STUDY AND RESULTS

This section details a case study addressing a H.264/AVC decoder, exposing firstly how all application and platform model parameters are setup, here from concrete measurements (these could be also determined using estimators, at the expense of accuracy), and secondly the results of previously described exploration flow based on their use. This will additionally lead to a better valuation of DPR usefulness, potential energy efficiency benefits and conditions of effectiveness.

A. H.264/AVC decoder

The application which is considered in this validation study is a H.264/AVC profile video decoder specification modified to comply with parallel software (multicore) / hardware (reconfigurable) execution. An ESL design methodology [22] is used to provide real implementations for the possible hardware functions, which serve as an entry point to the exploration flow of Section 4. The input specification code used is a version derived from the ITU-T reference code [24] to better cope with hardware design constraints.

The deblocking filter (DB_Filter), inverse CAVLC (Inv_CAVLC), and inverse quantization and transform block (Inv_QTr) contribute together to 76% of the global execution time on a single CPU core. They represent the three functionalities of the decoder that can be either software or hardware executed.

In addition to these acceleration opportunities, we aim at exploring solutions mapped onto parallel architectures including multicore CPUs. For this, we consider a multithreaded version of the decoder exploiting the possibility of slice decomposition of frames supported in the H.264/AVC standard. Indeed a slice represents an independent zone of a frame, it can reference other slices of previous frames for decoding; therefore decoding one slice (of a frame) is independent from another (slice of the same frame). This way, the decoder can process different slices of a frame in parallel. We have thus considered a decomposition of the image where two streams process two halves of a same frame (Figure 5). The corresponding task graph is defined by $\mathcal{G}$ as:

$$\mathcal{G} \quad = \quad \{Exp\_Golomb, \ MB\_Header, \ Inv\_CAVLC_1, \\ Inv\_CAVLC_2, Inv\_QTr_1, \ Inv\_QTr_2, \ Inv\_Pred_1, \\ Inv\_Pred_2, \ DB\_Filter_1, \ DB\_Filter_2\}. \quad \textbf{(7)}$$

This graph can be deployed using up to six accelerators and two processors on the underlying platform. Accelerators are fully generated from a reference C code at this level in a way to derive precise performance, resource, and power information, and to define relevant reconfigurable regions for DPR execution (Table 4). Some functions are reported with two implementations (sequential and parallel resulting from HLS loop unrolling) to account for the impacts of parallelism on energy efficiency. Software tasks are characterized in a similar way by running the code on CPU cores to derive execution times and energy, possibly at the different supported frequencies (Table 5).

B. Target platform

The execution platform is based on two ARM CortexA8 cores and an eFPGA, assuming a Virtex-6 device model supporting DPR. Table 4 shows the corresponding platform parameters that have been set as exposed in Section C.2. The method of [18] is used to identify an optimal set of PRRs under performance and FPGA layout constraints, considering all the hardware implementations of tasks previously considered. Three PRRs of 1200, 3280 and 2000 slices were found to reduce slice and BRAM count from respectively 49% and 33% over a purely static implementation of all hardware tasks. Therefore this configuration is used as a basic PRR setup in the following deployment analysis.

From $P_{V6LX240T}^{empty} = 41.7 \ \mu W/slice$ measured previously on the device, it is possible to derive the empty power consumption

Table 4. Model parameters for a dual CortexA8/Virtex-6 LX240T potential platform.

Platform	N^{core}	N^{PRR}	N^{EU}	Description
	2	3	5	CortexA8/V6LX240T
Cores	EU_j	$F_{j,k}$ (MHz)	$P_{j,k}^{empty}/P_{j,k}^{run}$ (mW)	Description
	EU_1	600	24/445	core #1
	EU_2	600	24/445	core #2
PRRs	EU_j	$N_j^{cell}; N_j^{bram}; N_j^{dsp}$	P_j^{empty} (mW)	Description
	EU_3	$1200; 8; 0$	50	PRR #1
	EU_4	$3280; 8; 0$	137	PRR #2
	EU_5	$2000; 8; 0$	83	PRR #3
DPR	Conf. Ctlr	T^{1cell} (μs)	E^{1cell} (nJ)	Description
		0.41	61.5	UPaRC

for each defined PRR: $P_3^{empty} = 50\ mW$, $P_4^{empty} = 137\ mW$ and $P_5^{empty} = 83\ mW$. The empty power of CPU cores come from similar measurements on an OMAP3530 based development board: $P_{j,k}^{empty} = 24\ mW$ and $P_{j,k}^{run} = 445\ mW$ for a CortexA8 core at $F_{j,k} = 600MHz$.

Additionally, the reconfiguration controller used is an optimized IP called UPaRC supporting a reconfiguration speed of $400\ MB/s$ for a power of $P_{controller} = 150\ mW$ [20]. This corresponds to $T^{1cell} = 0.41\mu s$ and $E^{1cell} = 61.5mJ$ (Section C.2) from which reconfiguration time and energy of a PRR are easy to compute.

## C. Application model parameters

Hardware power models are based on the power consumed by the whole task implemented on a PRR. In our validation and model characterization approach, this power is measured (it could also be estimated) and therefore includes logic cells, DSP and BRAM blocks as well, if the corresponding hardware task makes use of such dedicated resources.

Table 5 shows the application model parameters in details for the H.264 decoder example. The decoder is composed of ten tasks among which six can be run in hardware. All tasks are characterized in terms of software and hardware mapping following the generation and measurement procedure of Section C.3.

For each hardware task (T_5, T_6, T_9, T_{10}), two versions of different cost and performance tradeoffs are produced using HLS loop level parallelism. Therefore, if we consider the example of Inv_QTr_1 (T_5), three implementations $T_{5,1}$, $T_{5,2}$, $T_{5,3}$ are possible with respectively 5.10ms (CortexA8 600MHz), 2.46 ms (hardware #1) and 1.97 ms (hardware #2 with loop unrolling). For each of the two hardware implementations, three possible PRR mappings are described along with the associated energy cost (computed as shown in C.3). This realistic characterization of different task implementations based on practical data improves the reliability of estimations and exploration results, which are addressed in the following.

D. Exploration results and analysis

Under previous conditions of application, SoC architecture and dynamic reconfiguration, the primary output of the exploration flow is plotted in Figure 6. It is worth noting first the very important quantity of solutions analyzed, over 1 million possible mappings are evaluated for this design. This exploration example is processed in a matter of seconds with an Intel Core i5 based workstation.
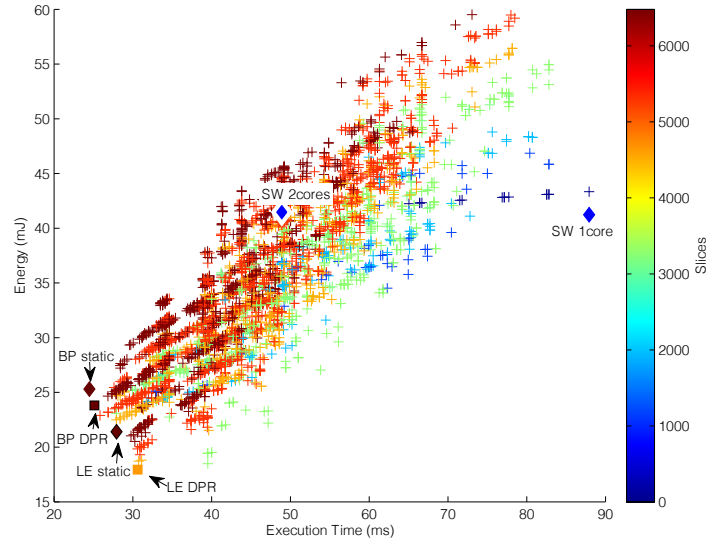
Fig. 6. Energy vs. execution time exploration results. Colors represent the number of FPGA resources (slices) of a solution.

Six solutions are highlighted from the results: (i) full software implementation using one CPU core (*SW_1Core*), (ii) full software execution using two cores (*SW_2Cores*), (iii) the lowest energy solution using *static* accelerators (*LE_Static*), (iv) the best performance solution using *static* accelerators (*BP_Static*), (v) the lowest energy solution using dynamic reconfiguration (*LE_DPR*) and (vi) the best performance solution using dynamic reconfiguration (*BP_DPR*). Details of these characteristic solutions are summarized in table 6. Since *SW_1Core* is almost twice slower for the same energy compared to *SW_2Cores*, *SW_2Cores* is considered as a reference result in the following to let the comparison of relative improvements from hardware accelerated solutions. To further help this analysis, exploration results also output scheduling, allocation and power profiles that are illustrated in figures 7 and 8 for *BP_Static*, *LE_Static*, *BP_DPR* and *LE_DPR*.

We can firstly note that the four accelerated solutions perform better compared to the reference software execution, both in terms of performance and energy. Hardware significantly improves processing efficiency while offloading CPU cores which results in 50% faster execution and 39% energy savings at the global decoder application level. Dynamic reconfiguration introduces a slight performance penalty due to reconfiguration

Table 5. Task parameters for an H.264/AVC decoder application.

T_i	$T_{i,k}$	$I_{i,j,k}=1$	$C_{i,j,k}$(ms)	$E_{i,j,k}$(mJ)	$P^{idle}_{i,k}/P^{run}_{i,k}$(mW)	$N^{cell}_{i,k}; N^{bram}_{i,k}; N^{dsp}_{i,k}$	Description
T_1	$T_{1,1}$	$I_{1,1,1}$ $I_{1,2,1}$	5.00	2.23	24/445	–	Exp_Golomb
T_2	$T_{2,1}$	$I_{2,1,1}$ $I_{2,2,1}$	4.92	2.19	24/445	–	MB_Header
T_3	$T_{3,1}$	$I_{3,1,1}$ $I_{3,2,1}$	11.03	4.91	24/445	–	Inv_CAVLC_1
	$T_{3,2}$	$I_{3,4,2}$	7.45	1.46	55.1/4.4	3118; 6; 0	
T_4	$T_{4,1}$	$I_{4,1,1}$ $I_{4,2,1}$	11.03	4.91	24/445	–	Inv_CAVLC_2
	$T_{4,2}$	$I_{4,2,4}$	7.45	1.46	55.1/4.4	3118; 6; 0	
T_5	$T_{5,1}$	$I_{5,1,1}$ $I_{5,2,1}$	5.10	2.27	24/445	–	Inv_QTr_1
	$T_{5,2}$	$I_{5,3,2}$	2.46	0.24	34.2/11.47	1056; 7; 0	
	$T_{5,2}$	$I_{5,4,2}$	2.46	0.45	34.2/11.47	1056; 7; 0	
	$T_{5,2}$	$I_{5,5,2}$	2.46	0.32	34.2/11.47	1056; 7; 0	
	$T_{5,3}$	$I_{5,3,3}$	1.97	0.21	42.2/12.87	1385; 7; 0	
	$T_{5,3}$	$I_{5,4,3}$	1.97	0.38	42.2/12.87	1385; 7; 0	
	$T_{5,3}$	$I_{5,5,3}$	1.97	0.27	42.2/12.87	1385; 7; 0	
T_6	$T_{6,1}$	$I_{6,1,1}$ $I_{6,2,1}$	5.10	2.27	24/445	–	Inv_QTr_2
	$T_{6,2}$	$I_{6,3,2}$	2.46	0.24	34.2/11.47	1056; 7; 0	
	$T_{6,2}$	$I_{6,4,2}$	2.46	0.45	34.2/11.47	1056; 7; 0	
	$T_{6,2}$	$I_{6,5,2}$	2.46	0.32	34.2/11.47	1056; 7; 0	
	$T_{6,3}$	$I_{6,3,3}$	1.97	0.21	42.2/12.87	1385; 7; 0	
	$T_{6,3}$	$I_{6,4,3}$	1.97	0.38	42.2/12.87	1385; 7; 0	
	$T_{6,3}$	$I_{6,5,3}$	1.97	0.27	42.2/12.87	1385; 7; 0	
T_7	$T_{7,1}$	$I_{7,1,1}$ $I_{7,2,1}$	5.39	2.40	24/445	–	Inv_Pred_1
T_8	$T_{8,1}$	$I_{8,1,1}$ $I_{8,2,1}$	5.39	2.40	24/445	–	Inv_Pred_2
T_9	$T_{9,1}$	$I_{9,1,1}$ $I_{9,2,1}$	17.49	7.78	24/445	–	DB_Filter_1
	$T_{9,2}$	$I_{9,3,2}$	1.57	0.14	33.4/6	686; 5; 0	
	$T_{9,2}$	$I_{9,4,2}$	1.57	0.28	33.4/6	686; 5; 0	
	$T_{9,2}$	$I_{9,5,2}$	1.57	0.19	33.4/6	686; 5; 0	
	$T_{9,3}$	$I_{9,4,3}$	1.55	0.29	40.3/7.4	1869; 5; 0	
	$T_{9,3}$	$I_{9,5,3}$	1.55	0.20	40.3/7.4	1869; 5; 0	
T_{10}	$T_{10,1}$	$I_{10,1,1}$ $I_{10,2,1}$	17.49	7.78	24/445	–	DB_Filter_2
	$T_{10,2}$	$I_{10,3,2}$	1.57	0.14	33.4/6	686; 5; 0	
	$T_{10,2}$	$I_{10,4,2}$	1.57	0.28	33.4/6	686; 5; 0	
	$T_{10,2}$	$I_{10,5,2}$	1.57	0.19	33.4/6	686; 5; 0	
	$T_{10,3}$	$I_{10,4,3}$	1.55	0.29	40.3/7.4	1869; 5; 0	
	$T_{10,3}$	$I_{10,5,3}$	1.55	0.20	40.3/7.4	1869; 5; 0	

delays, however the best performance solution based on DPR is only 2.6% slower than a static implementation. In terms of energy, the lowest energy solution using DPR is 57% more efficient than the reference *SW_2Cores* and 16% more energy efficient than a static implementation.

Inspecting the schedule and resources usage of figures 7 and 8 emphasizes the fact that performance solutions make use of a maximum of resources, while low energy implementations tend to use less execution units and improve their utilization rate. For example, the energy of *BP_Static* is reduced by offloading the execution of function *CAVLC* from the first CPU core to PRR2, which results in an energy gain of 3.9 *mJ* (−15%) for a performance penalty of 3.4 *ms* (+14%). The same applies for DPR implementation *BP_DPR* in which Core1 and PRR3 can be removed to save 5.9 *mJ* (−25%) while increasing execution time by 5.5 *ms* (+22%). Minimizing the number of reconfigurations (represented in red in the scheduling profiles) is also an important factor impacting execution time and energy consumption. In the DPR solutions of the decoder, the configuration of PRR2 is kept to execute two consecutive instances of *Inv_CAVLC*, and the

same applies for the execution of *DB_Filter* on PRR1. However, *Inv_QTr* is mapped to PRR1 for the first instance and to PRR2 for the second. Execution dependencies between *DB_Filter* and *Inv_QTr* do not allow to save a reconfiguration of *Inv_QTr* without a penalty on global execution time, impacting also energy. The second instance of *Inv_QTr* is thus executed on PRR2.

In terms of DPR benefits over static implementation, the H.264 decoder example shows that DPR brings 16% energy improvement for 31% FPGA resource (slice) reduction and an execution time increase of 10%. Energy gains come from the reduction of the static area of the programmable logic and the associated idle power, decreasing from 318 *mW* to 210 *mW* (34%). These results help evaluating the practical benefits of dynamic reconfiguration, considering also that there is room for improvement on the H.264 decoder by moving more functions to hardware.

Finally, it is also interesting to note that for this application, none of the four hardware solutions highlighted exploits PRR blanking. In the *LE_DPR* solution, hardware execution units are not free for a sufficient period of time to compensate the energy

Table 6. Highlights of exploration results.

Implementation results	$Energy(mJ)$	$T_{EX}(ms)$	$CPUs$;	$Slices$;	$DSPs$;	$BRAMs$
SoftWare 1core	41.23	87.92	1;	0;	0;	0
SW 2cores(reference)	41.47	48.92	2;	0;	0;	0
Lowest Energy - static	21.40 (-48%)	27.93 (-43%)	1;	6480;	0;	18
Best Performance - static	25.30 (-39%)	**24.49 (-50%)**	2;	6480;	0;	18
Lowest Energy - DPR	**17.94 (-57%)**	30.62 (-37%)	1;	4480;	0;	16
Best Performance - DPR	23.84 (-43%)	25.13 (-49%)	2;	6480;	0;	24
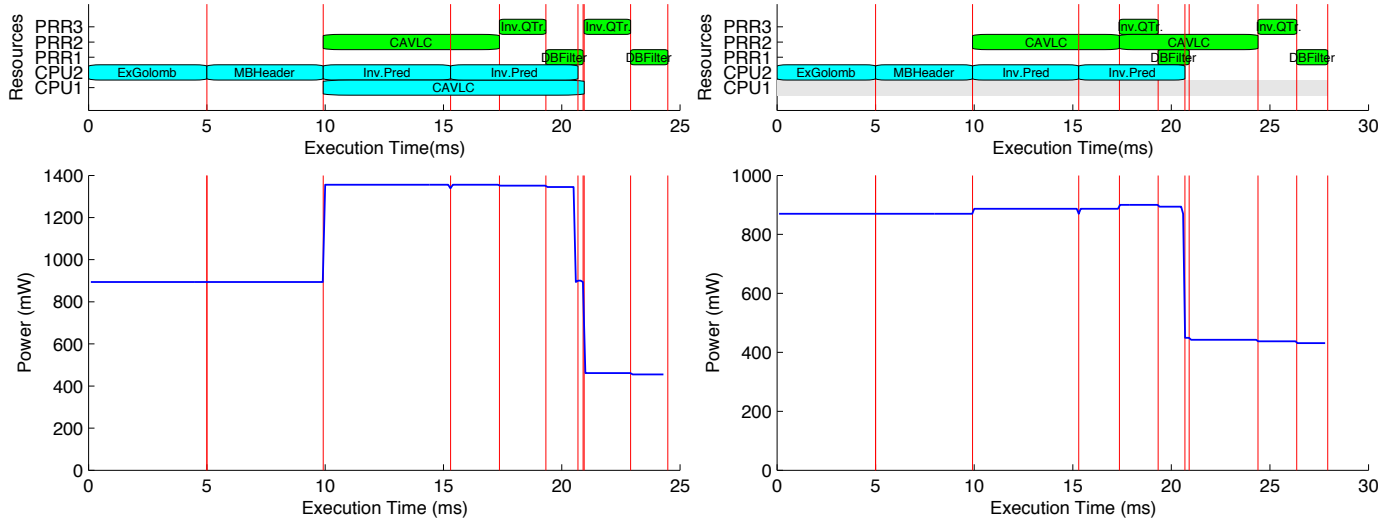
Fig. 7. Scheduling and power profile of *BP_Static* (left) and *LE_Static* (right) solutions.

overheads implied by PRR reconfigurations. Therefore these estimations provide a possible assessment to know whether or not to use blanking in a design.

The end result from a potential platform made of two CPUs and a FPGA fabric is a solution based on a single core execution with dynamic reconfiguration of six hardware accelerated functions on two PRRs. The corresponding implementation represents 57% and 37% performance and energy improvements over a dual core software execution, which is also 16% more energy efficient over a static hardware implementation of the same accelerators with 10% less performance.

6. CONCLUSION AND PERSPECTIVES

This paper addressed the evaluation of the interest of dynamic and partial reconfiguration in the context of low power optimizations. Indeed, the possibility to reduce area (by reusing the same resources for several sequential tasks) is an interesting approach to save static power and/or to use a smaller FPGA. But this capability doesn't come for free, and this paper proposes a complete formalism of tasks execution on a platform based on processor cores and reconfigurable area. This formalism is then used as a support for design space exploration including tasks mapping in the different available execution resources. Previous detailed results report different potential energy efficiency improvements on a representative video processing application. DPR benefits are sensitive over pure software (dual core) execution with 57% energy gains for 37% better performance. There are comparatively less limited benefits against static (no DPR) hardware acceleration with 16% energy gains, but for 10% less performance (resulting from the overheads of reconfiguring partial regions). In addition to these numbers, we can derive a set

of conditions that are essential for practical DPR effectiveness. First, the cost of reconfiguration is high both in terms of delay and energy. Thus all reconfiguration overheads have to be minimized as much as possible, which means to support high speed reconfiguration control and to reach a schedule minimizing the number of reconfigurations. Second, hardware execution being to a very large extent significantly more energy efficient than software, accelerated functions are likely to be employed. On top of this, minimizing the number of regions will improve the results, both because it reduces the inherent power (especially the idle power), but also because it improves usage of the available regions. Therefore, there is still room for improving the H.264 decoder, in which only three functions are considered for acceleration, as quality of results will grow when increasing and sharing the number of hardware functions on a limited number of regions.

From these considerations, a first perspective is to address further energy gains with the definition of run-time scheduling policies supporting energy-aware execution of dynamic hardware and software tasks. Indeed exploration is likely to provide overestimated performances at design time since it has to be based on (static) worst case execution times. Therefore, there is room for complementary energy savings by exploiting dynamic slacks resulting from lesser execution times at run-time, and these scheduling decisions can benefit from the same models used for mapping exploration. Finally, another direction of research will be to build an Operating System, on this exploration and scheduling base, to achieve efficient cooperation with existing processor level techniques (e.g. DVFS) and converge towards an advanced heterogeneous power management scheme.
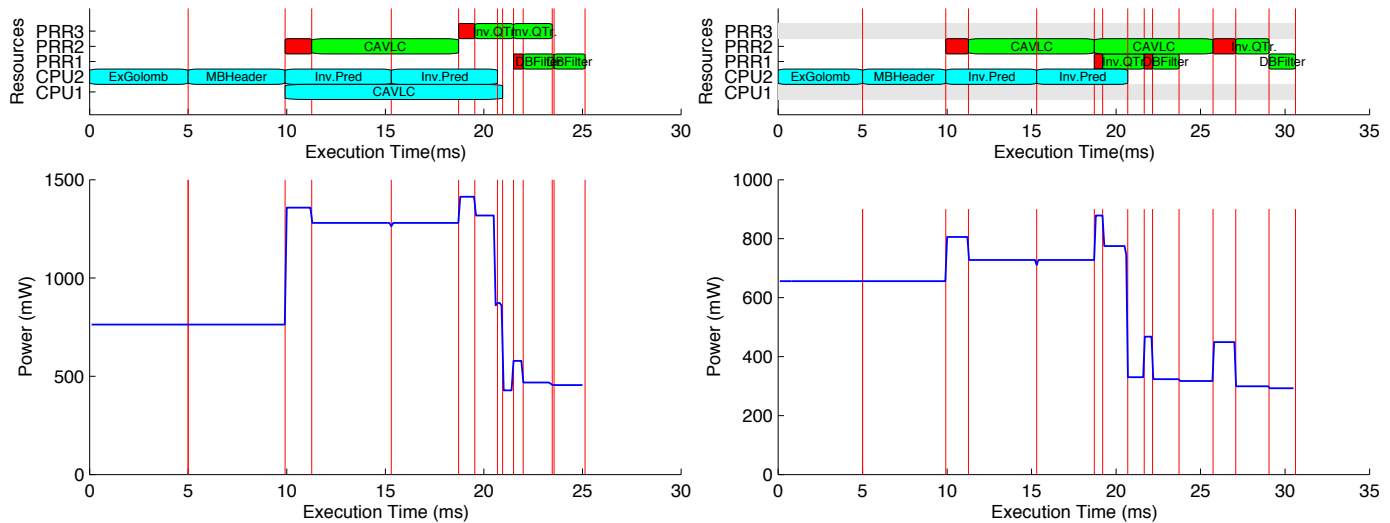
Fig. 8. Scheduling and power profile of *BP_DPR* (left) and *LE_DPR* (right) solutions.

REFERENCES

1. James G. Eldredge and Brad L. Hutchings. 1996. Run-Time Reconfiguration: A Method for Enhancing the Functional Density of SRAM-based FPGAs. *Journal of VLSI Signal Processing* 12, 1 (1996), 67–86.

2. Kashif Latif, Arshad Aziz, and Athar Mahboob. 2011. Deciding equivalances among conjunctive aggregate queries. *Computers & Electrical Engineering* 37 (2011), 1043 – 1057.

3. Ian Kuon and Jonathan Rose. 2007. Measuring the gap between FPGAs and ASICs. *Computer-Aided Design of Integrated Circuits and Systems, IEEE Transactions on* 26 (2007), 203–215.

4. A. Amara, F. Amiel, and T. Ea. 2006. FPGA vs. ASIC for low power applications. *Microelectronics Journal* 37 (2006), 669 – 677.

5. F. Palumbo, C. Sau, and L. Raffo. 2015. Coarse-grained reconfiguration: dataflow-based power management. *IET Computers & Digital Techniques* 9 (2015), 36 – 48.

6. B. López, J. Valverde, E. de la Torre, and T. Riesgo. 2014. Power-aware multi-objective evolvable hardware system on an FPGA. *NASA/ESA Conference on Adaptive Hardware and Systems (AHS)* (2014), 61 – 68.

7. A. Rodriguez, J. Valverde, and E. de la Torre. 2015. FPGA vs. ASIC for low power applications. *International Conference on ReConFigurable Computing and FPGAs (ReConFig)* (2015), 1 – 7.

8. T. Tuan and B. Lai. 2003. Leakage power analysis of a 90nm FPGA. In *IEEE Custom Integrated Circuits Conference*. DOI: http://dx.doi.org/10.1109/CICC.2003.1249359

9. L. Sterpone, L. Carro, D. Matos, S. Wong, and F. Fakhar. 2011. A new reconfigurable clock-gating technique for low power SRAM-based FPGAs. In *Design, Automation & Test in Europe Conference & Exhibition (DATE)*. 1–6.

10. Qiang Wang, Subodh Gupta, and Jason H. Anderson. 2009. Clock power reduction for virtex-5 FPGAs. In *Proceedings of the ACM/SIGDA International Symposium on Field Programmable Gate Arrays*. 13–22.

11. Katarina Paulsson, Michael Hubner, and Jurgen Becker. 2009. Dynamic power optimization by exploiting self-reconfiguration in Xilinx Spartan 3-based systems. *Microprocessors and Microsystems* 33 (2009), 46 – 52.

12. T.T.-O. Kwok and Yu-Kwong Kwok. 2006. Practical design of a computation and energy efficient hardware task scheduler in embedded reconfigurable computing systems. In *Proceedings IEEE 20th International Symposium on Parallel and Distributed Processing, IPDPS*.

13. H. Kalte and M. Porrmann. 2005. Context saving and restoring for multitasking in reconfigurable systems. In *Proceedings IEEE International Conference on Field Programmable Logic and Applications*. 223–228. DOI: http://dx.doi.org/10.1109/FPL.2005.1515726

14. Ping-Hung Yuh, Chia-Lin Yang, Chi-Feng Li, and Chung-Hsiang Lin. 2009. Leakage-aware task scheduling for partially dynamically reconfigurable FPGAs. *ACM Transactions on Design Automation of Electronic Systems, TODAES* 14, 4 (2009), 1–26. DOI: http://dx.doi.org/10.1145/1562514.1562520

15. Shaoshan Liu, Richard Neil Pittman, and Alessandro Forin. 2010. Energy reduction with run-time partial reconfiguration. In *Proceedings ACM/SIGDA International Symposium on Field Programmable Gate Arrays*. 292–292.

16. Robin Bonamy, Daniel Chillet, Olivier Sentieys, and Sébastien Bilavarn. 2011. Parallelism Level Impact on Energy Consumption in Reconfigurable Devices. *ACM SIGARCH Computer Architecture News* 39 (2011), 104–105.

17. Robin Bonamy, Sébastien Bilavarn, Daniel Chillet, and Olivier Sentieys. 2014. Power Consumption Models for the Use of Dynamic and Partial Reconfiguration. *Microprocessors and Microsystems, Elsevier* (2014).

18. François Duhem, Fabrice Muller, Robin Bonamy, and Sébastien Bilavarn. 2015. FoRTReSS: a flow for design space exploration of partially reconfigurable systems. *Design Automation for Embedded Systems, Springer Verlag ,* (2015).

19. J. Kriegel, F. Broekaert, A. Pegatoquet, and M. Auguin. 2010. Power optimization technique applied to real-time video application. In *Proc. 13th Sophia Antipolis Microelectronics Forum (SAME)*. Sophia Antipolis, France, University Booth.

20. R. Bonamy, H-M. Pham, S. Pillement, and D. Chillet. 2012. UPaRC - Ultra Fast Power aware Reconfiguration Controller. In *Design, Automation & Test in Europe Conference & Exhibition (DATE)*.

21. Xilinx, Inc. 2010. *UG360 – Virtex-6 FPGA Configuration User Guide (v3.1)*. Technical Report.

22. Taheni Damak, Imen Werda, Sébastien Bilavarn, and Nouri Masmoudi. 2013. Fast Prototyping H.264 Deblocking Filter Using ESL tools. *Transactions on Systems, Signals & Devices, Issues on Communications and Signal Processing* 8, 3 (Dec. 2013), 345–362.

23. E. Senn, D. Chillet, O. Zendra, C. Belleudy, R. Ben Atitallah, A. Fritsch, and C. Samoyeau. 2012. Open-People: an Open Platform for Estimation and Optimizations of energy consumption. In *Design and Architectures for Signal and Image Processing Conference (DASIP 2012), 23/10/2012, Karlsruhe, Germany*.

24. ITU-T 2005. Advanced Video Coding for Generic Audio-visual Services. *ISO/IEC 14496-10, ITU-T Recommendation H.264*, Version 4, (2005).

BIOGRAPHIES

Robin BONAMY received his M.E. degree in Electronics and Embedded Systems in 2009 and the Ph.D. degree from University of Rennes, France, in 2013. His research interests are reconfigurable devices, power and energy models and design space exploration especially for energy consumption reduction. He is currently focused on low power, wireless devices and he is consultant in innovation based on digital electronic technologies.

   Sébastien BILAVARN received the B.S. and M.S. degrees from the University of Rennes in 1998, and the Ph.D. degree in electrical engineering from the University of South Brittany in 2002 (at formerly LESTER, now Lab-STICC). Then he joined the Signal Processing Laboratories at the Swiss Federal Institute of Technology (EPFL) for a three year post-doc fellowship to conduct research with the System Technology Labs at Intel Corp., Santa Clara. Since 2006 he is an Associate Professor at Polytech'Nice-Sophia school of engineering, and LEAT Laboratory, University of Nice-Sophia Antipolis - CNRS. His research interests are in design, exploration and optimization from early specifications with investigations in heterogeneous, reconfigurable and multiprocessor architectures, on a number of french, european and international collaborative research projects.

   Daniel Chillet is member of the Cairn team which is an Inria team located between Lannion and Rennes in France. He received the Engineering degree and the M.S. degree in electronics and signal processing engineering from University of Rennes 1, respectively, in 1992 and in 1994, the Ph.D. degree in signal processing and telecommunications from the University of Rennes 1 in 1997, and the habilitation to supervise PhD in 2010. He is currently a Professor of electrical engineering at Enssat, engineering school of University of Rennes 1. Since septembre 2014, he is director of the master "Information and Communication Technology" of the University of Science and Technology of Hanoi. His research interests include memory hierarchy, reconfigurable resources, real-time systems, and middleware. All these topics are studied in the context of MPSoC design for embedded systems. Low power design based on reconfigurable systems is one important topic and spatio-temporal scheduling, memory organization and operating system services have been previously addressed on several projects.

   Olivier SENTIEYS joined University of Rennes (ENSSAT) and IRISA Laboratory, France, as a full Professor of Electronics Engineering, in 2002. He is leading the CAIRN Research Team common to INRIA Institute (national research institute in computer science) and IRISA Lab. (research institute in computer science and random systems). Since September 2012 he is on secondment at INRIA as a Senior Research Director. His research activities are in the two complementary fields of embedded systems and signal processing. Roughly, he works firstly on the definition of new System-on-Chip architectures, especially the paradigm of reconfigurable systems, and their associated CAD tools, and secondly on some aspects of signal processing like finite arithmetic effects and cooperation in mobile systems. He is the author or coauthor of more than 150 journal publications or peer-reviewed conference papers and holds 5 patents. He is the head of the "Architecture" department of IRISA.